Synthesis of Gelatin Nanoparticles via Simple Coacervation

Article *in* Journal of Surface Science and Technology · January 2005

CITATIONS
19

READS
515

4 authors, including:

Biswaranjan Mohanty
Monash University (Australia)
46 PUBLICATIONS **622** CITATIONS
SEE PROFILE

Vinod K Aswal
Bhabha Atomic Research Centre
472 PUBLICATIONS **6,937** CITATIONS
SEE PROFILE

J. Surface Sci. Technol., Vol 21, No. 3-4, pp. 149-160, 2005

Synthesis of Gelatin Nanoparticles via Simple Coacervation

BISWARANJAN MOHANTY[a], V. K. ASWAL[b], J. KOHLBRECHER[c] and H. B. BOHIDAR[a,*]

[a]*School of Physical Sciences, Jawaharlal Nehru University, New Delhi-110067, India*
[b]*Solid State Physics Division, Bhabha Atomic Research Centre, Mumbai-400085, India*
[c]*Paul Scherrer Institute, CH-5232 Villigen, Switzerland.*

Abstract — Dynamic light scattering (DLS), Transmission electron microscopy (TEM) and Small Angle Neutron Scattering (SANS) experiments are performed on biodegradable gelatin nanoparticles for size measurements and stability analysis. Though gelatin nanoparticles were previously prepared by the desolvation method [1], the simple coacervation [2] process is being proposed as a new and simple method to prepare very small and stable nanoparticles. Gelatin nanoparticles were found to have spherical conformation by transmission electron microscopy having a typical diameter 45 ± 5nm, which was supported by dynamic light scattering data. This is very small compared to the same reported earlier for this polypeptide (~ 200nm). Electrophoresis measurement showed that the nanoparticles present in the supernatant are negatively charged.

Keywords : *Gelatin, nanoparticle, light and neutron scattering, transmission electron microscopy and electrophoresis.*

INTRODUCTION

Nanoscience has been a subject of considerable interest because of the special properties associated with nanoparticles, such as large surface to volume ratio, increased surface reactivity as compared to bulk material and their porous or core shell structure. Nanoparticles have been around since Michael Faraday's time of 1857 when he first developed the gold colloidal particles. Its regime has broadened spanning three decades, and research on various methods of their preparation and applications is still in progress. In pharmaceutics, biodegradable and biocompatible

*Author for correspondence E-mail : bohi0700@mail.jnu.ac.in
Paper presented at *International Conference on Soft Matter* (ICSM 2004), Kolkata, India, Nov. 18–20.

polymeric nanoparticles have shown great potential as drug carriers. Compared to other colloidal carriers, like liposome, biopolymers represent better stability when in contact with biological fluids, and their polymeric nature allows one to obtain the desired controlled and sustained release of the entrapped drug molecules [3-7]. Nanoparticles represent drug delivery systems suitable for most of the administration routes, even if a rapid recognition by the immune system limits their use as injectable carriers. These were initially devised as carriers for vaccines and anti-cancerous drugs [8]. Nanoparticles made of gelatin (a denatured protein) biopolymers have the potential to be used as drug or gene delivery carriers. Gelatin is readily available, has a relatively low antigenicity and is in use in a number of parenteral formulations [9].

Gelatin is a natural macromolecule obtained from collagen. It is a polyampholyte having both cationic and anionic groups along with hydrophobic groups. This biopolymer is polypeptide with the representation – $(Gly - X - Pro)_n$ where X represents the amino acid, mostly lysine, arginine, methionine and valine ~ 6%. As per Merck technical data, one third of the chain is comprised of glycine ~33% and another one third is either proline or hydroxyproline ~33%. The rest are other residues. The gelatin molecule is ~13% positively charged (lysine and arginine), ~12% negatively charged (glutamic and aspartic acid) and ~11% of the chain hydrophobic in nature (comprising leucine, isoleucine, methionine and valine). Glycine, proline and hydroxyproline form the rest of the chain. The positive : negative : hydrophobic segments are present in the approximate ratio 1 : 1 : 1, which makes this polypeptide special.

Coacervation is a process during which a homogeneous solution of charged macromolecules undergoes liquid-liquid phase separation, giving rise to a polymer rich dense phase at the bottom and a transparent solution (supernatant) above. These two liquid phases are incompatible, immiscible and are in equilibrium. In simple polyelectrolyte coacervation, addition of salt or alcohol normally promotes coacervation [2, 10]. The dilute liquid phase, the supernatant (rich in nanoparticles) could be characterized by dynamic laser light scattering (DLS), small angle neutron scattering (SANS), transmission electron microscopy (TEM) and electrophoresis measurements, which forms the objective of our present work.

EXPERIMENTAL

Materials : Undeuterated ethanol (C_2H_5–OH) was obtained from Merck, Germany and deuterated ethanol (C_2H_5–OD) was obtained from Sigma (for SANS studies to minimize incoherent background). Gelatin (Type-B, bovine skin extract,

microbiology grade devoid of E. coli and liquefier presence, nominal molecular weight ≈ 90 ± 10 kD) was bought from E. Merck, India. All other chemicals used were bought from Thomas Baker, India.

Methods : *Sample preparation* — The solvent used was deionized water for DLS and D_2O for SANS. The pH (using 0.1 M HCl) was first set as per the experimental requirement and the gelatin solutions (1% w/v) were prepared by dispersing gelatin in this medium at 60°C. The ionic strength was kept at zero in our experiments. The macromolecule was allowed to hydrate completely; this took 30 min to 1 hour. Initially at room temperature, the solution pH was 5.15 ± 0.01. Three drops of HCl were added to set the pH at 5 ± 0.05, which is the iso-electric point [2] of the type-B gelatin. This formed the stock solution. The stock solution was titrated with ethanol and the titration profiles clearly established the transition points in terms of the percentage of volume of ethanol (V) added relative to that of the solvent corresponding to the first occurrence of turbidity at V_t = 44 ± 2 % (v/v) and a sharp point of inflection at V_p = 46 ± 2 %(v/v), where the turbidity attained its maximum value. Addition of more ethanol drove the system towards the precipitation point. The values of V_t and V_p characterized the initiation of intermolecular folding and intra molecular aggregate formation of the charge neutralized gelatin molecules, and the subsequent micro coacervate droplet formation [2]. The turbid phase separated into two liquid phases, the dense phase (coacervate) at the bottom and the diluted phase (supernatant) at the top through high-speed centrifugation (relative centrifugal force ~ 6637g) at the ethanol concentration larger than V_t but less than V_p (not at V_p, where precipitation occurs). Then the supernatant was collected by pasture pipette from the top of the centrifuge cells and were used for different experiments.

Analysis of DLS measurement — The particle size measurements were done by dynamic laser light scattering (DLS) technique, using a 90 Plus Particle Size Analyzer from Brookhaven Instruments Corp. (BIC), USA and an indigenous goniometer. The excitation source was a 35 mW He-Ne laser emitting at a wavelength of 632.8 nm in linearly polarized single frequency mode, which was focused onto the sample cell and the scattered light was detected by a photo-multiplier tube (Hamamatsu). The signal was converted into intensity auto-correlation function by a digital correlator. The scattering angle was fixed at 90° and the data analysis was done using CONTIN software provided by Brookhaven Instruments. This technique was used to get the size of the particles. The details of the DLS experiment and the process of data analysis are reported elsewhere [11, 12].

Analysis of SANS measurement – SANS is a diffraction technique, which involves scattering of a monochromatic beam of neutrons from the sample and measuring the scattered neutron intensity as a function of the scattering angle. The small angle neutron scattering (SANS) experiments were performed at the Swiss Spallation Neutron Source SINQ, Paul Scherrer Institute, Switzerland. The measurements were performed with a mean neutron wavelength of 0.8 nm at a sample-to-detector distance 2 m, 6 m and 15 m. An extended range for the magnitude of the scattering vector $q = 4 \pi \sin \theta / \lambda$ (where 2θ is the scattering angle and λ is the neutron wavelength) from $0.03\ nm^{-1} \leq q \leq 3.4\ nm^{-1}$ was covered by three combinations of the above-mentioned sample-to-detector distances. The scattered neutron intensity was recorded with a two-dimensional 96 cm × 96 cm detector. The samples were kept in stoppered quartz cells (Hellma, Germany) with a path length of 1 mm. The neutron spectra of water were also measured in a 1 mm path length quartz cell. The raw spectra were corrected for background, sample cell, and electronic noise by conventional procedures [13-15]. Furthermore, the two dimensional isotropic scattering spectra data were azimuthally averaged and converted to absolute scale using the incoherent scattering data of pure water. Dilute systems are ideally suited for studying the shapes and sizes of the particles. In these systems, particle concentration is very low. The intensity of the scattered neutrons [16, 17], I (q) can be written as

$$I(q) = n(\rho_p - \rho_m)^2 V^2 \exp\left(\frac{-q^2 R_g^2}{3}\right) \quad (1)$$

Here, $(\rho_p - \rho_m)^2$ is referred to as the contrast factor, n is the number of particles per unit volume of the sample; V is the average volume of a single particle.

Analysis of TEM measurement — Average particle size, size distribution and morphology were examined by Fei-Philips Morgagni 268D transmission electron microscope (Digital TEM with image analysis system and Maximum Magnification = × 2, 80,000) at a voltage of 100 kV. The aqueous dispersion of the particles was drop-cast onto a carbon coated copper grid and grid was air dried at room temperature (25^oC) before loading on the microscope.

Analysis of Electrophoresis measurement — Electrophoresis measurement was performed on a zeta potential instrument (ZC-2000, Microtec, Japan). In order to minimize the influence of electrolysis on the measurements, molybdenum (+) and platinum (–) plates were used as electrodes. Also, during the measurements, the cell chamber tap on molybdenum electrode was kept open to release the air

bubbles for the purpose of reducing their effects on the particle movement. During the measurements, the molybdenum anode was cleaned each time as it turned from a metallic to blue-black colour.

RESULTS AND DISCUSSION

Table 1 shows the time dependent stability of gelatin nanoparticles observed through dynamic light scattering measurement. It shows that the particles were quite stable at room temperature ~ 25°C over a period of two months. The DLS data showed an average size of about ~ 45.9 nm (mean diameter by CONTIN analysis) and the average effective diameter (mean diameter by cumulant analysis) ~ 30.44 nm with an average polydispersity ~ 0.3. For DLS measurement we have used the solvent viscosity = 2.8 cP and refractive index =1.342, which refers to ethanol concentration (44 ± 2 v/v %).

TABLE 1

Particle size determination by DLS through two techniques.

Time/days	Diameter by CONTIN analysis/nm	Effective Diameter/nm	Polydispersity
0	51 ± 5	30 ± 3	0.22
10	43 ± 5	30 ± 3	0.35
20	50 ± 5	34 ± 3	0.27
30	44 ± 5	31 ± 3	0.27
60	42 ± 5	27 ± 3	0.38

The cumulant analysis yields a very specific ratio of moments of the particle number distribution. If N(R) is the particle number distribution, the cumulant analysis yields the ratio of the 6th to 5th moment of N(R) given by [11,12],

$$R_{Cumulant} = \frac{\int N(R)R^6 dR}{\int N(R)R^5 dR} = \frac{<R^6>}{<R^5>} \quad (2)$$

The CONTIN algorithm calculates either the volume distribution, P (V(R)) = N(R) R^3 or an intensity distribution, P (I(R)) = N(R) R^6. The average of the CONTIN

result is defined as

$$R_{CONTIN} = \frac{\int P(V(R))RdR}{\int P(V(R))dR} = \frac{<R^4>}{<R^3>} \quad (3)$$

which is the ratio of the 4th moment to the 3rd moment of N(R)

$$\text{or} \quad \frac{\int P(I(R))RdR}{\int P(I(R))dR} = \frac{<R^7>}{<R^6>} \quad (4)$$

which is the ratio of 7th to 6th moment of N(R). In all the cases the cumulant and the CONTIN analysis will give different values as long as the size distribution is broad alike in our case (polydispersity ~ 0.3). The CONTIN method yields better results since it is insensitive to baseline fluctuations unlike the cumulant method that yields the effective diameter values [12]. These are compared in Table 1. It can be clearly seen that the cumulant method under estimates the size significantly. The large polydispersity can be ascribed to the polydispersity inherent in gelatin samples [18].Table 2 shows the combination of data from Dynamic light scattering (DLS), small angle neutron scattering experiments (SANS) and transmission electron microscopy (TEM).

TABLE 2

Average particle size of gelatin particles.

Techniques	Diameter of nanoparticle/nm
DLS	~ 46 ± 2
SANS	~ 51 ± 2
TEM	~ 48 ± 2

Plot of I(q) vs. q in Fig. 1 shows the scattering in supernatant samples at temperature 25°C. A plot of the logarithm of scattering intensity, I(q) versus q^2 will be a straight line fitting to Eq.(1) in the small q region ($q < 3R_g^{-1}$) and the slope gives the radius of gyration, R_g ~ 20.5 nm (Fig. 2). By assuming the shape

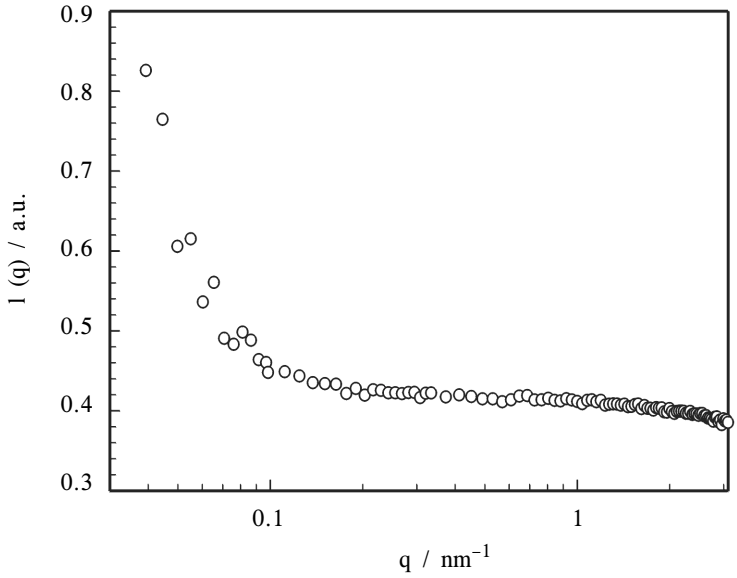

Fig. 1. SANS data for supernatant performed at 25 ^{o}C. Plot of scattering intensity (I) versus wide range of Log(q), (0.03 nm^{-1} ≤ q ≤ 3.5 nm^{-1}).

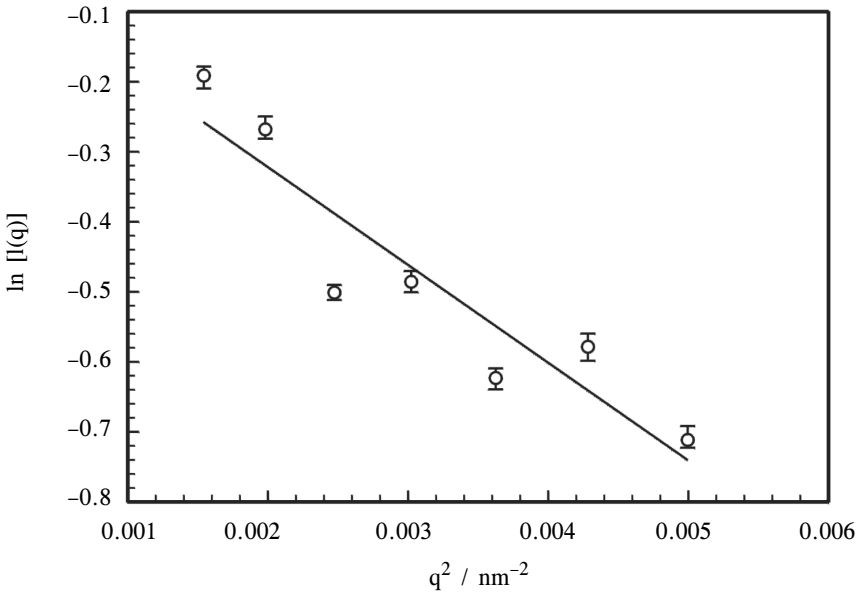

Fig. 2. SANS data for supernatant, Guinier logarithmic plot of scattering intensity versus q^2 (q ≤ 0.07nm^{-1}).

of particle to be a sphere, we have converted the radius of gyration, R_g into a particle radius, R through

$$R = \sqrt{\frac{5}{3}} R_g \tag{5}$$

It was estimated that the radius of the particle is ~ 26 nm and the particle size (diameter) is 52 ± 2 nm, comparable to the size measured by DLS. TEM data (Fig. 3) shows that the gelatin particles have diameters in the range of 45nm to 90nm. Larger particles (~ 90 nm) seen in the TEM picture could arise due to the aggregation on the substrate surface. Though the TEM picture shows the large variation of particle sizes, In Table 2, we have shown only the average particles range in the order of 48 ± 2 nm. Secondly, TEM sample preparation involved drying of the supernatant on the grid at ambient temperature. There is a lot of discussion usually of what the drying effects are on the fluctuational organic nanoparticles as they are in a state of non-equilibrium during drying and as a result alter their shape and size considerably. Mostly, freeze fracture or cryo-TEM is usually performed to establish such structures. At the time of electrophoresis measurement, the particles (moving in Brownian motion in bulk) were viewed in a microscope (× 500) fitted with a reticule through optical dispersion of a laser beam. A voltage of 50V was applied during the measurement and the particle migration was noted to be stable. The result of average zeta potential value and the corresponding electrophoretic mobility was –23.9 mV and 0.422 um/sec*cm/V.

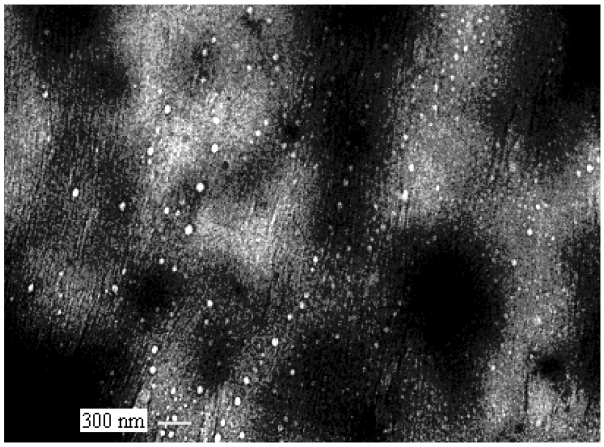

Fig. 3. TEM picture of a supernatant sample at concentration 44 ± 2% (v/v), pH= 5 at T = 25 ^{o}C after staining. Particles of sizes 48nm, 65 nm and 90 nm are clearly seen in the picture.

The surface charge distribution was found to be negative as the zeta potential was negative. We have only shown the representative data on frequency (no. of particles) vs. zeta potential of gelatin nanoparticles in the supernatant medium (Fig. 4). Smoluchowski's formula was used to calculate the zeta potential. The equation is described as follows [19].

$$\zeta = \frac{4\pi\eta}{\varepsilon} \times \mu \times 9 \times 10^7 \tag{6}$$

where ζ = Zeta potential (mV), η = Viscosity of solution (0.028 poise), ε = Dielectric constant (56.4) and μ = Electrophoretic mobility (0.422 μm/sec*cm/V). The value of viscosity and dielectric constant were taken at ethanol concentration 44 ± 2 %(v/v).

For a neutral sample, for which the ensemble average charge asymmetry is equal to zero, concentrating the samples leads to the formation of a supernatant containing counterions and almost neutral globules while the precipitate at the bottom remains neutral [20]. For samples with asymmetric charge distributions, the supernatant contains highly charged globules while the precipitates are neutral [20].

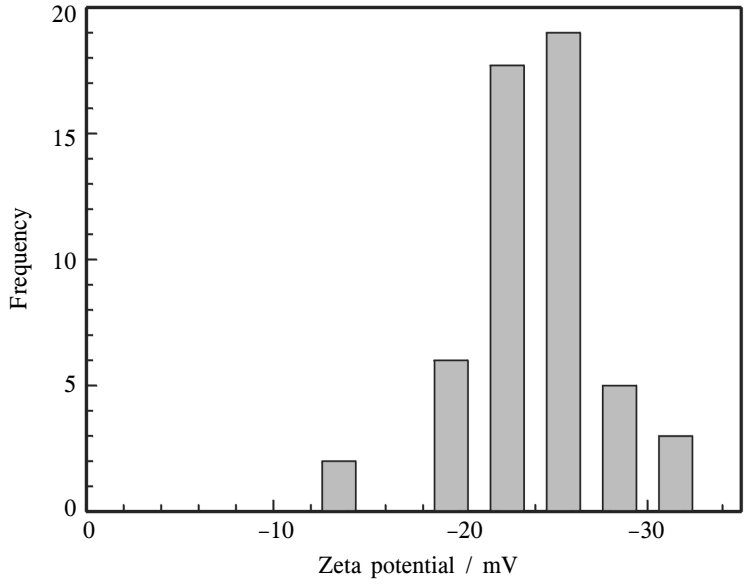

Fig. 4. Electrophoresis measurement of gelatin nanoparticle in supernatant medium at pH =5 at 25 ^{O}C.Plot of zeta potential vs. frequency is shown.

In our experimental data, the particles in supernatant carried negative charge which confirms that the solution initially had asymmetric charge distributions. We have argued earlier that the possibility of particle contraction due to ethanol-induced dehydration results in contraction of random coil particles into hard nano-spheres [21].

In coacervation, the high molecular weight fraction of gelatin (aggregates of size $\sim$ 200 nm) goes to the coacervate phase. Low molecular weight species formed the nanoparticles of diameter $\approx$ 50 nm in the supernatant [21]. The objective of specifying the difference of molecular weight is to account for the effect of polydispersity inherent in gelatin samples though the weight average molecular weight was $\approx 90 \pm 10$ kD. So the removal of the high molecular weight gelatin fraction by coacervation process enabled the enhancement of stability of these particles. The physical mechanism of aggregation can be visualized as follows. Gelatin is not soluble in alcohols whereas water is a good solvent. As ethanol is added to water, the water molecules will preferentially bind to the alcohol molecules through hydrogen bonding and the resultant binary mixture becomes a marginal solvent for gelatin molecules. Furthermore, it has been shown that the binary liquid mixture of ethanol and water exhibit maximum hydrogen bonding at ethanol concentration = $44 \pm 2\%$ v/v which is supported by thixotropic and viscosity data [18]. The prepared gelatin nanoparticles showed high stability in water and ethanol binary mixture (at concentration $\sim 44 \pm 2\%$v/v), which forms the dispersion medium. Particle stability is also enhanced by presence of ethanol in the supernatant phase because contamination due to bacteria is avoided significantly. It was evident from DLS, SANS and TEM studies that the particles showed neither sedimentation nor flocculation and the particle size remained constant during the investigation time of two months.

CONCLUSION

Coacervation is a new method by which we could get very stable nanoparticles around 45 nm which was confirmed through DLS, SANS and TEM experiments (see Table 2). Electrophoresis measurement confirms the particles are negatively charged. However, we believe that this not only provides us with new information about nanoparticle but also has consequences that reach beyond nanosciences. Previously, the concepts of polymer physics has had an enormous impact on the understanding of structural and dynamic properties of coacervation, but we are now in a position to return this favour and use supernatant as ideal model system for "equilibrium polyelectrolytes". It must be realized that the experimental studies

with highly hydrogenous polyelectrolyte systems using SANS has suffered weak scattering power, which makes it impossible to produce data with a sufficient accuracy over a required wave vector range from diluted supernatant solutions.

ACKNOWLEDGMENT

B.M is thankful to Council of Scientific and Industrial Research, India for a Senior Research Fellowship. We also gratefully acknowledge Paul Scherrer Institute, Switzerland for allowing us to perform neutron scattering. This work was supported by the DST (Govt. of India) Nanoscience and Technology initiative.

REFERENCES

1. C. Coester, H. Von Briesen, K. Langer and J. Kreuter, Gelatin Nanoparticles by Two Step Desolvation - A New Preparation Method, Surface Modifications and Cell Uptake. J. Microencapsul., 17, 187 (2000).
2. B. Mohanty and H. B. Bohidar, Biomacromolecules, 4, 1080 (2003).
3. P. Couvreur, B. Kante, L. Grislain, M. Roland and P. T. Speiser, J. Pharm. Sci., 71, 790 (1982).
4. J. Kreuter, Pharm. Acta. Helv., 53, 33 (1978).
5. G. Lambert, E. Fattal and P. Couvreur, Adv. Drug. Deliv. Rev., 47, 99 (2001).
6. S. M. Moghimi, L. Illum and S. S. Davis, Crit. Rev. Ther. Drug. Carrier. Syst., 187 (1990).
7. G. J. Russell-Jones, J. Control Release, 65, 49 (2000).
8. V. P. Torchilin, J. Microencapsul., 15, 1 (1998).
9. A. Hassig and K. Stampfli, Bibliotheca Haematologica, 33, 1 (1969).
10. H. G. Bungenberg de Jong, 'In Colloid Science', Vol II : Ed.; H. R. Kruyt, Elsevier, New York (1949).
11. B. J. Berne and R. Pecora, 'Dynamic Light Scattering'; NY: Wiley (1976).
12. H. B. Bohidar, 'In Handbook of Polyelectrolytes'; Vol-II, Ed.; H. S. Nalwa, American Scientific Publishers, California (2002).
13. B. Jacrot, G. Zaccai, Biopolymers, 20, 2413 (1981).
14. M. Ragnetti, R. C. Oberthür, Colloid Polym. Sci., 264, 32 (1986).
15. G. D. Wignall and F. S. Bates, J. Appl. Crystallogr., 20, 28 (1987).
16. G. L. Squires, Thermal Neutron Scattering; Cambridge University Press, Cambridge (1978).

17. L. A. Feigin and D.I.Svergun, 'Structure Analysis by Small-Angle Neutron X-Ray Scattering and Neutron Scattering'; Plenum Press, New York (1987).
18. H. B. Bohidar and B. Mohanty, Phys. Rev., E, 69, 021902 (2004).
19. M. von Smoluchowski, Z. Phys. Chem., 92, 129 (1918).
20. A. V. Dobrynin, R. H. Colby and M. Rubinstein, J. Polym. Sci. Part B : Poly. Phys., 42, 3513 (2004).
21. B. Mohanty, V. K. Aswal, P. S. Goyal and H. B. Bohidar, PRAMANA- J. Phys., 63, 271 (2004).